JOURNAL OF SOLID STATE CHEMISTRY 68, 73–87 (1987)

Crystal Structure and Electrical Conductivity of the "One-Dimensional" Solid Electrolyte *N,N*-Dimethylmorpholinium Pentaiodotetraargentate

XIE SISHEN* AND S. GELLER

Department of Electrical and Computer Engineering, University of Colorado, Boulder, Colorado 80309

Received April 16, 1986

The new solid electrolyte *N,N*-dimethylmorpholinium pentaiodotetraargentate, $[(CH_3)N(CH_2)_2(CH_2)_2O]Ag_4I_5$ ($DMMAg_4I_5$), has a crystal structure which allows the Ag^+ ions to move effectively in only one dimension. The channels for this motion result from the sharing of opposite faces of icosahedra, having iodides at their centers, forming infinite chains of icosahedra along the *a* axis. The joining of the icosahedra forms three more face-sharing tetrahedra at each junction, or a total of 23 tetrahedra per eight Ag^+ ions, which are distributed non-uniformly over the tetrahedral sites. The limited number of pathways for the Ag^+ ion diffusion leads to a low average conductivity, $1 \times 10^{-4}\ \Omega^{-1}\ cm^{-1}$ and a high activation enthalpy, 0.35 eV. Crystals of $DMMAg_4I_5$ belong to space group $P2_12_12_1$ (D_2^4) with $a = 13.167(4)$, $b = 23.437(3)$, $c = 12.758(3)$ Å; the unit cell contains eight formula units. The structure of dimethylmorpholinium iodide (DMMI) confirms the chair model for the DMM^+ ion. Crystals of DMMI belong to space group $P2_1/m$ (C_{2h}^2), with $a = 8.861(4)$, $b = 8.020(2)$, $c = 6.685(2)$ Å, $\beta = 101.07(3)°$; each unit cell contains two formula units.

1. Introduction

This paper will be indicative of a return, in this laboratory, to studies of AgI-based solid electrolytes, after several years devoted to Cu^+ ion conductors. Our studies involve, always, the relation of the conductivity to the structure of the solid electrolyte. This has been the case since the study of $RbAg_4I_5$ (*1*) in which it was first shown that the origin of the electrolytic conductivity was directly related to the structure. The main features are the face sharing of the iodide polyhedra to form passageways through which the Ag^+ ions move, a substantial ratio of available sites for the Ag^+ ions to these charge carriers, and a non-uniform distribution of charge carriers over crystallographically nonequivalent sets of sites. These features are common to every Cu^+- and Ag^+-halogenide solid-electrolyte structure determined earlier than and subsequent to that of $RbAg_4I_5$ (*2–17*).

Some time ago, it was inferred directly from the crystal structure of $(C_5H_5NH)_5Ag_{18}I_{23}$ that it was a "two-dimensional" solid electrolyte (*5*). Subsequently, Hibma confirmed this inference by conductivity measurements on single crystals at room temperature (*18*). This is still the only two-dimensional solid electrolyte among those that are double salts of silver iodide or cuprous halogenides.

* On leave from Institute of Physics, Chinese Academy of Sciences, Beijing, China.

0022-4596/87 $3.00

Recently we have found a new solid electrolyte in which the Ag^+ ions are constrained to move effectively in a single direction. At present, this is inferred entirely from the crystal structure which we report here together with the results of conductivity measurements on polycrystalline material. We hope eventually to obtain single crystals large enough for directional conductivity measurements.

2. Experimental

The crystal on which the data were collected had an orthorhombic morphology in the crystal class 222. The largest dimensions were 0.38, 0.34, and 0.26 mm along a, b, and c, respectively. Several secondary faces were not included in the approximation of the crystal shape by a 12-face polyhedron for the absorption corrections, which were calculated on an $8 \times 8 \times 8$ grid basis.

Initial diffraction data were obtained with a Buerger precession camera (Mo$K\alpha$ radiation). Reflections $h00$, $0k0$, $00l$ were absent for h, k, l odd, implying $P2_12_12_1$ as the most probable space group.

The X-ray data used for the structure determination were collected with a Nicolet P3/F autodiffractometer in the range $3 \leq 2\theta \leq 55°$ with Mo$K\alpha$ radiation and bent graphite monochromator. Scan rates were in the range 2 to 30° per minute. The intensities of four particular reflections were checked after each 100 reflections measured. Of a possible 5012 independent reflections observable in the 2θ range, 2555 were observed ($F^2 > 3\sigma(F^2)$) and used in the structure determination and refinement. The measured spacings of 25 reflections were used for the determination of the lattice constants by least-squares calculations. The results were $a = 13.167(4)$, $b = 23.437(3)$, $c = 12.758(3)$ Å.

The crystal used for the structure determination was grown by G. P. Espinosa by the gel technique about 16 years ago. The gel was made by first dissolving 23.3 g $Na_2SiO_3 \cdot 9H_2O$ in 100 ml of water and then acidifying to pH 4 with 50% aq. nitric acid. Very small amounts of NaI were added to a mixture of 0.486 g of *N,N*-dimethylmorpholinium iodide and 4.290 g AgI in 30 ml of water until all were completely dissolved. The mixture was then poured slowly into a test tube two-thirds full of gel. Small crystals of the compound grew slowly as the solution diffused into the gel. (The above is all the recorded information available.) The process is a slow exsolution of the compound as dilution proceeds.

We have also found that small crystals can be obtained if the polycrystalline material (see below) is melted at just above its melting point (~220° C) for about 5 min and then slowly cooled.

To make the polycrystalline specimens, stoichiometric amounts of *N,N*-dimethylmorpholinium iodide and silver iodide were ground together in an agate mortar. The mixture was then compressed into a pill, which was put into a Pyrex tube. The tube was flushed with dry N_2; the N_2 pressure was reduced to 0.5 atm, after which the tube was sealed off and placed in an oven at 140° C for 24 hr. The specimen was then removed from the tube, reground, repelletized, enclosed in a Pyrex tube with 0.5 atm N_2 as before, and heated again at 140°C for 24 hr. This was repeated once, after which an X-ray powder diffraction photograph was taken of the material, showing, in two cases, that the procedure was satisfactory; i.e., phase-pure material was produced.

The *N,N*-dimethylmorpholinium iodide used to prepare the specimens was synthesized and purified (mp = 253–255.5°C) in the laboratory of B. B. Owens, who kindly sent us some several years ago, and the AgI was supplied by PCR Research Chemicals, Inc.

The formula weight of the compound is

1182.18; the volume of the unit cell is 3937(3) Å^3; with eight $[(CH_3)_2N(CH_2)_2$-$(CH_2)_2O]Ag_4I_5$ per unit cell, and the calculated density is 3.99 g cm^{-3}. The density was measured roughly by compressing 2.63 g of polycrystalline material into a cylindrical pill of diameter 0.958 cm and length 0.941 cm, giving 3.89 g cm^{-3}. The linear absorption coefficient for Mo$K\alpha$ radiation is 116.4 cm^{-1}. Lorentz-polarization corrections were also made.

The method of preparation of the cell for conductivity measurement was similar to that described in Ref. (*19*). The device used for the conductivity measurements is shown in Fig. 1 of Ref. (*20*). Impedance measurements were made with a Hewlett–Packard 4274A multifrequency LCR meter. Those reported here were taken at 200 Hz, at which the imaginary contribution to the impedance was negligible.

For simplicity in later discussion, we shall use "DMM" to mean *N,N*-dimethylmorpholinium.

3. Electrical Conductivity

The results of the conductivity-vs-temperature measurements are plotted (Fig. 1) as $\log_{10}(\sigma T)$ vs $10^3\ T^{-1}$, with $240 \leq T \leq 340$ K. The data lie on a straight line, which gives for the enthalpy of activation of motion, h_m, of the Ag^+ ions, 0.35 eV. At 298 K, the conductivity is $1.0 \times 10^{-4}\ \Omega^{-1}\ cm^{-1}$ and at 340 K, it is $4.7 \times 10^{-4}\ \Omega^{-1}\ cm^{-1}$.

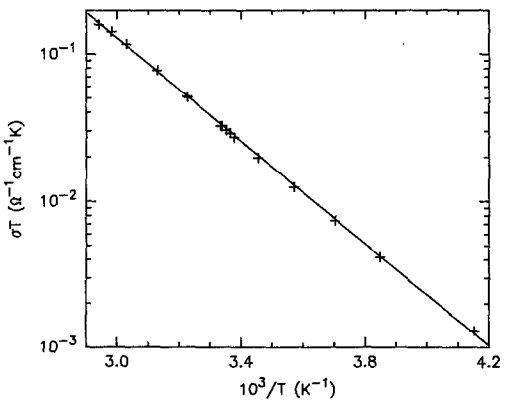

FIG. 1. $\log_{10}$ (conductivity × temperature) vs reciprocal temperature of polycrystalline $DMMAg_4I_5$.

At temperatures of 340 K or higher, the resistivity of the cell increases with time. This has occurred for four different specimens. When cells heated above 340 K are cooled to room temperature, the measured resistivity is usually at least five times higher than original. A cell heated to only 320 K had the same resistivity at room temperature that it had before heating.

A powder photograph of the solid electrolyte in the cell after heating above 340 K, shows no change. Similarly, a powder photograph of the electrode material does not indicate the presence of phases other than silver and the solid electrolyte.

Single-crystal photographs taken at 363 and 408 K with a Buerger precession camera do not indicate a phase change, nor were there any qualitatively observable changes in intensities.

We can only speculate that a reaction takes place at the solid electrolyte–electrode interface, causing the formation of a very thin layer of insulating material. Eventually, it may be possible to resolve this problem when single crystals of a size suitable for conductivity measurements are obtained.

4. Determination and Refinement of the Structure

The general and only positions in space group $P2_12_12_1$ are x, y, z; $\frac{1}{2} - x, \bar{y}, \frac{1}{2} + z$; $\bar{x}, \frac{1}{2} + y, \frac{1}{2} - z$; $\frac{1}{2} + x, \frac{1}{2} - y, \bar{z}$. Thus the asymmetric unit contains two formula units, or two DMM, $8Ag^+$, and 10 I^- ions. All ten I^- ion positions were given directly by MULTAN. Then it was a reasonably simple matter to calculate approximately all the possible positions that the Ag^+ ions

could occupy. The structure of a dimethylmorpholinium compound had not been determined. However, a "chair" structure for morpholine had been deduced (*21*) from NMR spectra. This was sufficient to consider such a model for the DMM ion. (Subsequently, this was confirmed by a structure analysis of DMMI which is described in the Appendix.)

Difference synthesis was used to locate the DMM ions and restrained least-squares calculations and subsequently, trial-and-error and least-squares calculations were used to improve atom positions. Similarly least-squares and trial-and-error calculations were used to obtain the Ag^+ ion distribution. There was some difficulty because of high correlations among thermal parameters and multipliers of the Ag^+ ions.

In the final least-squares cycle, all parameters of the light atoms, the (isotropic) thermal parameters of Ag8, 9, and 19, and positional parameters and multipliers of Ag5, 9, and 22 were held constant. A total of 228 parameters, including scale factor and extinction coefficient, were varied. The extinction coefficient, g, which the program applies to the F_{calc} as $(F_c)\,(1 + gI_c)^{-1}$, where I_c is the calculated intensity, converged to 5.779×10^{-8}. For the iodides, four of the values of |shift/error| were 0.01; the rest were 0.00. For the Ag^+ ions, the values ranged from 0.00 to 0.07. For the 2555 observed reflections, $R = \Sigma\,||F_{obs}| - |F_{calc}||/\Sigma|F_{obs}| = 0.050$.[1] Calculations were also done on the enantiomorph; the two are indistinguishable.

There were 198 correlation coefficients with absolute values greater than 0.5; 23 were greater than 0.90 and three were equal to 0.99. Our programs (probably like most or all others) calculate only covariances, and therefore only pair correlations, but the behavior of the results of the least-squares calculations indicated that there must also be multiple correlations (*22*), as commonly occurs in the related solid electrolyte structures. The parameters that were held constant in the final least-squares cycle were not always held constant, just as in calculations for other solid electrolytes and other structures in which strong parameter correlations (*23, 24*) occur. For *true* convergence, *all* possible variable parameters must be allowed to vary in the final cycle (*23*). However, long experience with such structures has borne out an earlier suggestion (*25, 26*) that even with the highest quality data, high correlations might prevent it. Nevertheless, the impossibility of *true* convergence does not preclude the *essential* correctness of the structure that has such troubles.

There is a good reason for assigning an isotropic thermal parameter to the Ag^+ ions in the Ag8, 9, and 19 sites; their occupancies are very low, equivalent to 5.5 electrons for Ag19, for example (Table I).

To conserve space, the parameter table for the light atoms is deposited with the F_c vs F_0 tables.[1] This table includes the parameters for the H atoms, which did contribute significantly to several structure amplitudes. The total number of light atoms in the asymmetric unit is 44 with a total of 176 parameters including 44 isotropic thermal parameters, set to 7.00 Å^2.

The final results of the refinement are given in Table I (multipliers, positional parameters and the equivalent isotropic thermal parameters, B_{eqv}) and Table II (thermal parameters $U_{ij} = \beta_{ij}/2\pi^2 a_i^* a_j^*$). A table with

[1] See NAPS document No. 04442 for 28 pages of supplementary material. Order from ASIS/NAPS. Microfiche Publications, P.O. Box 3513, Grand Central Station, New York, NY 10163. Remit in advance $4.00 for microfiche copy or for photocopy, $7.75 up to 20 pages plus $.30 for each additional page. All orders must be prepaid. Institutions and Organizations may order by purchase order. However, there is a billing and handling charge for this service of $15. Foreign orders add $4.50 for postage and handling, for the first 20 pages, and $1.00 for each additional 10 pages of material, $1.50 for postage of any microfiche orders.

TABLE I

POSITIONAL AND THERMAL PARAMETERS OF HEAVY ATOMS

Atom	Multiplier	x	y	z	$B_{eqv}(Å^2)$
I1	1	0.1617(2)	0.41249(9)	0.3143(2)	3.87(4)
I2	1	0.1515(2)	0.08426(9)	0.2984(2)	4.26(4)
I3	1	0.3117(2)	0.2486(1)	0.1344(2)	4.36(4)
I4	1	0.2258(2)	0.24436(9)	0.4934(2)	3.92(4)
I5	1	0.4894(2)	0.14802(9)	0.3850(2)	3.82(4)
I6	1	0.2950(2)	0.40876(9)	0.6914(2)	4.22(4)
I7	1	0.3025(2)	0.06932(9)	0.6421(2)	4.19(4)
I8	1	0.4663(2)	0.35714(9)	0.4104(2)	3.92(4)
I9	1	0.4776(2)	0.24119(9)	0.7410(2)	4.17(4)
I10	1	0.1577(2)	0.2288(1)	0.8409(2)	4.25(4)
AG1	0.285(8)	0.2579(9)	0.3704(5)	0.4873(9)	6.1(3)
AG2	0.627(7)	0.1921(5)	0.3682(2)	0.5152(4)	6.3(1)
AG3	0.0	0.0743	0.3195	0.4212	
AG4	0.0	0.0053	0.2506	0.4845	
AG5	0.288	0.037(1)	0.1671(7)	0.386(1)	8.2(4)
AG6	0.0	0.1655	0.1277	0.5065	
AG7	0.621(7)	0.2835(4)	0.1277(2)	0.4457(4)	5.7(1)
AG8	0.154(7)	0.406(2)	0.167(1)	0.590(2)	7.00
AG9	0.100	0.481	0.251	0.516	7.00
AG10	0.0	0.377	0.311	0.593	
AG11	0.271(7)	0.174(1)	0.2073(5)	0.276(1)	5.9(3)
AG12	0.299(7)	0.2850(9)	0.1731(5)	0.319(1)	6.4(3)
AG13	0.0	0.3845	0.2513	0.3436	
AG14	0.278(6)	0.2794(9)	0.3162(4)	0.3167(9)	5.3(2)
AG15	0.552(8)	0.1947(6)	0.2952(3)	0.2875(6)	8.4(2)
AG16	0.945(7)	0.1681(3)	0.1583(2)	0.6622(4)	7.26(9)
AG17	0.0	0.2910	0.1889	0.6806	
AG18	0.846(7)	0.2804(3)	0.2903(2)	0.7016(4)	6.6(1)
AG19	0.132(8)	0.699(2)	0.195(1)	0.310(2)	7.00
AG20	0.0	0.0702	0.2427	0.6428	
AG21	0.786(7)	0.4742(4)	0.1444(2)	0.6086(4)	6.6(1)
AG22	0.693	0.4855(4)	0.3492(2)	0.6303(4)	5.8(1)
AG23	0.937(8)	0.4726(3)	0.2553(2)	0.2838(3)	6.69(9)

Note: For this case, $B_{eqv} = (4/3)*(a^2*Beta(1,1) + b^2*Beta(2,2) + c^2*Beta(3,3) + 2*a*c*Beta(1,3)*cosBeta)$

TABLE II

THERMAL PARAMETERS, U_{ij}

Name	U(1,1)	U(2,2)	U(3,3)	U(1,2)	U(1,3)	U(2,3)
I1	0.050(1)	0.046(1)	0.051(1)	0.0042(9)	0.003(1)	0.001(1)
I2	0.050(1)	0.053(1)	0.058(1)	0.006(1)	-0.006(1)	-0.011(1)
I3	0.056(1)	0.060(1)	0.050(1)	0.002(1)	-0.001(1)	-0.000(1)
I4	0.066(1)	0.0402(9)	0.042(1)	0.0016(9)	0.003(1)	-0.0028(9)
I5	0.049(1)	0.048(1)	0.048(1)	0.0004(9)	-0.003(1)	0.002(1)
I6	0.054(1)	0.054(1)	0.052(1)	-0.003(1)	-0.007(1)	-0.006(1)
I7	0.055(1)	0.049(1)	0.056(1)	0.0040(9)	0.004(1)	0.010(1)
I8	0.054(1)	0.049(1)	0.047(1)	0.003(1)	-0.003(1)	-0.001(1)
I9	0.057(1)	0.044(1)	0.057(1)	-0.002(1)	-0.001(1)	-0.001(1)
I10	0.058(1)	0.054(1)	0.049(1)	-0.006(1)	0.003(1)	0.002(1)
AG1	0.090(7)	0.082(7)	0.061(6)	-0.019(6)	-0.007(6)	0.006(6)
AG2	0.116(4)	0.069(3)	0.053(3)	-0.004(3)	-0.019(3)	0.000(2)
AG5	0.13(1)	0.11(1)	0.074(8)	0.026(9)	0.013(8)	0.003(8)
AG7	0.073(3)	0.074(3)	0.068(3)	-0.001(2)	-0.014(3)	-0.006(3)
AG11	0.096(8)	0.054(5)	0.073(7)	-0.018(5)	0.016(7)	-0.001(5)
AG12	0.078(6)	0.072(5)	0.092(8)	-0.026(5)	0.008(6)	-0.024(6)
AG14	0.082(6)	0.062(5)	0.058(6)	0.026(5)	0.016(6)	0.006(5)
AG15	0.146(6)	0.092(4)	0.082(4)	0.041(4)	0.029(5)	0.006(4)
AG16	0.084(2)	0.108(3)	0.084(2)	0.033(2)	-0.000(2)	-0.013(2)
AG18	0.093(3)	0.073(2)	0.084(3)	-0.014(2)	0.004(2)	0.011(2)
AG21	0.103(3)	0.082(3)	0.066(2)	-0.011(3)	0.003(3)	-0.011(2)
AG22	0.078(2)	0.081(3)	0.062(3)	-0.013(2)	-0.004(2)	0.013(2)
AG23	0.114(3)	0.062(2)	0.079(2)	-0.001(2)	-0.015(2)	0.003(2)

the axial lengths of the root-mean-square vibration ellipsoids is also deposited with NAPS.[1]

5. Description and Discussion of the Structure

The crystal structure of $DMMAg_4I_5$ "tells" us that it is a one-dimensional conductor. In the Refs. (*2–17*), it has been well established that the most important requirements for a solid electrolyte are channels or passageways formed by face-sharing polyhedra and a substantial excess of these polyhedra over available charge carriers. The equilibrium sites for the charge carriers usually lie within the polyhedra, although in some cases, they could be very close to one of the faces.

In the structure of $DMMAg_4I_5$, the I^- ions form icosahedra, at the centers of which there is also an I^- ion. Therefore each icosahedron contains 20 tetrahedra. Each of two, and only two, faces at opposite ends of each icosahedron, is shared with another icosahedron, thus forming an infinite chain of face-sharing icosahedra running along the *a* axis (Fig. 2). At the junctions of the icosahedra, three more tetrahedra are formed (Fig. 2, also see later), resulting in 23 crystallographically independent tetrahedra per asymmetric unit. Thus a unit-cell increment of a single chain of icosahedra has two icosahedra and six additional "joining" tetrahedra. There are effectively two such increments per unit cell related by the 2_1 axes parallel to the *c* axis (Fig. 3, Table I, and Ref. (*27*)).

In the projection of the structure down the *a* axis (Fig. 3), it is very clear that there are no channel links between the chains of icosahedra; there is no way for a Ag^+ ion to move from one chain of icosahedra to another. This projection also shows why the (010) plane is a crystal-cleavage plane.

There are eight Ag^+ ions in each asymmetric unit. The least-squares calculations gave a total of only 7.81 Ag^+ ions per asymmetric unit. However, there are seven tetrahedra (Table I) that are "empty." The remaining 0.19 Ag^+ ions may be distributed over these, with an average of about 0.03 Ag^+ ions per tetrahedron. In any case, the approximate *limits of error* on the sum are ± 0.4.

We now look at the structure in more detail. Table III gives the distances between the central iodide ion and the other twelve iodide ions in the icosahedron. There are only 10 iodide ions in the asymmetric unit; thus the twofold screw axes cause each of three of the iodides to be represented in the icosahedron twice.

Table IV gives quantitative information

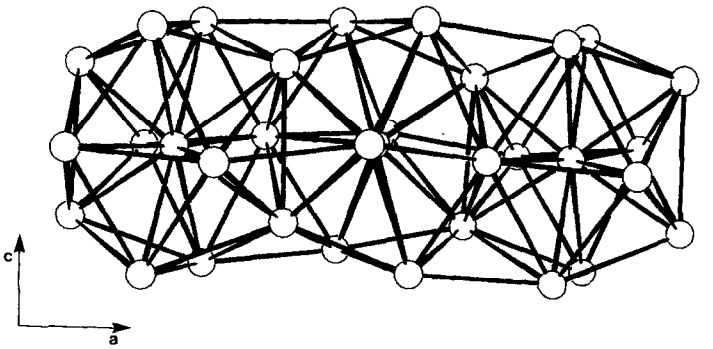

FIG. 2. Perspective drawing of the face-sharing icosahedra looking almost up the *b* axis. Only iodide ions are shown.

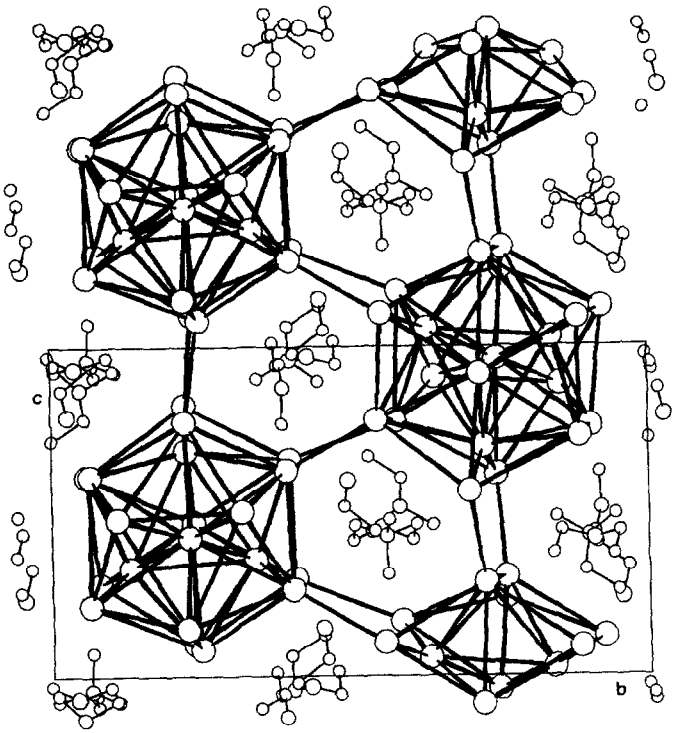

FIG. 3. Projection of the structure down the *a* axis. Silver ions are not shown.

on the tetrahedra, including the jump distances labeled Ag–Ag. In the first column under Ag site, those with an asterisk are the empty ones; for each of these, the equilibrium position was taken as the geometric center of the iodide tetrahedron and there are consequently no calculated standard errors given for Ag–I or Ag–Ag distances involving these.

A stereoscopic drawing of the iodide icosahedra along the *a* axis (i.e., ~1.5*a*) looking approximately along the [011] direction, is shown in Fig. 4a. Figure 4b drawn exactly to the same scale is a stereoscopic drawing of all possible pathways for the Ag^+ ions, the circles repesenting the equilibrium positions. The two drawings are shown separately to avoid confusion. However, the interested reader might consider making a transparency of Fig. 4b to superpose on Fig. 4a, if required for improved understanding.

TABLE III

DISTANCES (Å), CENTRAL IODIDE (14) TO OTHER IODIDES IN THE ICOSAHEDRON

I1	4.632(3)	I7	4.632(3)
I2	4.607(3)	I8	4.259(4
I3	4.719(4)	I8′	4.341(3)
I5	4.366(3)	I9	4.581(4)
I5′	4.295(3)	I9′	4.442(4)
I6	4.697(3)	I10	4.538(4)
		Ave.	4.509(3)

Of the 23 tetrahedra three share only two faces with other tetrahedra, and twelve share only three faces with other tetrahedra. In both types the unshared faces "see" DMM ions. The three tetrahedra that share only two faces are Ag21, 22, 23 which result from the joining of the icosahedra. Three tetrahedra at each "end" of the icosahedron share a face with these "joining" tetrahedra (see Table IV and Fig. 4a) accounting for six of the eight tetrahedra that share four faces. The remaining two share faces

TABLE IV

DISTANCES (Å) IN AND VOLUMES (Å^3) OF THE IODIDE TETRAHEDRA

Ag Site	I-I			Av. I-I	Ag-I		Av. Ag-I	Ag-Ag			Vol.
1	1-4 4.632	4-6	4.697	4.482	1 2.73(2)	6 2.80(2)	2.86(2)	2 0.94			11.13
	1-6 4.509	4-8	4.259		4 2.98(2)	8 2.93(2)		10 2.49			
	1-8 4.389	6-8	4.405					14 2.54			
2	1-4 4.632	4-5'	4.295	4.527	1 2.794(9)	5'2.98(3)	2.88(2)	1 0.94			11.48
	1-5'4.677	4-6	4.697		4 2.949(7)	6 2.782(8)		3 2.27			
	1-6 4.509	5'-6	4.349					19 2.68			
3*	1-4 4.632	4-5'	4.295	4.581	1 2.82	5'2.82	2.82	2 2.27	21	1.61	11.05
	1-5'4.677	4-9'	4.442		4 2.82	9'2.82		4 2.02			
	1-9'4.399	5'-9'	5.042					15 2.40			
4*	4-5'4.295	5'-8'	4.921	4.676	4 2.91	8'2.91	2.91	3 2.02	20	2.20	11.76
	4-8'4.341	5'-9'	5.042		5'2.91	9'2.91		5 2.36			
	4-9'4.442	8'-9'	5.020					9 0.33			
5	2-4 4.607	4-8'	4.341	4.629	2 2.70(2)	8'2.81(2)	2.92(2)	4 2.36	22	0.80	11.51
	2-8'4.651	4-9'	4.442		4 3.37(2)	9'2.80(2)		6 2.47			
	2-9'4.715	8'-9'	5.020					11 2.49			
6*	2-4 4.607	4-7	4.632	4.642	2 2.85	7 2.85	2.85	5 2.47			11.72
	2-7 4.828	4-8'	4.341		4 2.85	8'2.85		7 1.74			
	2-8'4.651	7-8'	4.798					16 2.11			
7	2-4 4.607	4-5	4.366	4.626	2 2.755(6)	5 2.860(7)	2.846(7)	6 1.74			11.58
	2-5 4.823	4-7	4.632		4 2.903(6)	7 2.866(7)		8 2.62			
	2-7 4.828	5-7	4.497					12 1.94			
8	4-5 4.366	5-7	4.497	4.655	4 3.23(4)	7 2.75(3)	2.90(3)	7 2.62	21	1.07	11.70
	4-7 4.632	5-9	5.042		5 2.87(3)	9 2.76(3)		9 2.39			
	4-9 4.581	7-9	4.810					17 1.97			
9	4-5 4.366	5-8	4.921	4.698	4 3.23	8 2.83	2.97	4 0.33	13	2.53	11.94
	4-8 4.259	5-9	5.042		5 2.93	9 2.89		8 2.39			
	4-9 4.581	8-9	5.020					10 2.20			
10*	4-6 4.538	6-8	4.405	4.575	4 2.83	8 2.83	2.83	1 2.49	22	1.76	11.21
	4-8 4.259	6-9	4.648		6 2.83	9 2.83		9 2.20			
	4-9 4.581	8-9	5.020					18 1.94			
11	2-3 4.864	3-4	4.719	4.642	2 2.91(1)	4 2.99(1)	2.88(1)	5 2.49			11.74
	2-4 4.607	3-9'	4.684		3 2.73(1)	9'2.87(2)		12 1.75			
	2-9'4.715	4-9'	4.442					15 2.08			
12	2-3 4.864	3-4	4.719	4.665	2 2.74(1)	4 2.89(1)	2.87(1)	7 1.94			11.87
	2-4 4.607	3-5	4.610		3 2.97(1)	5 2.88(2)		11 1.75			
	2-5 4.823	4-5	4.366					13 2.27			
13*	3-4 4.719	4-5	4.366	4.612	3 2.84	5 2.84	2.84	9 2.53	23	1.39	11.33
	3-5 4.610	4-8	4.259		4 2.84	8 2.84		12 2.27			
	3-8 4.797	5-8	4.921					14 2.09			
14	1-3 4.852	3-4	4.719	4.615	1 2.74(1)	4 2.90(1)	2.85(1)	1 2.54			11.44
	1-4 4.632	3-8	4.797		3 2.85(1)	8 2.90(2)		13 2.09			
	1-8 4.389	4-8	4.259					15 1.28			
15	1-3 4.852	3-4	4.719	4.628	1 2.805(9)	4 2.913(9)	2.86(1)	3 2.40			11.61
	1-4 4.632	3-9'	4.684		3 2.717(9)	9'3.01(2)		11 2.08			
	1-9'4.399	4-9'	4.442					14 1.28			
16	4-7 4.632	7-8'	4.798	4.626	4 3.046(6)	8'2.838(5)	2.862(5)	6 2.11			11.59
	4-8'4.341	7-10	4.902		7 2.747(5)	10 2.818(5)		17 1.79			
	4-10 4.538	8'-10	4.547					20 2.37			
17*	4-7 4.632	7-9	4.810	4.646	4 2.85	9 2.85	2.85	8 1.97			11.72
	4-9 4.581	7-10	4.902		7 2.85	10 2.85		16 1.79			
	4-10 4.538	9-10	4.411					18 2.39			
18	4-6 4.697	6-9	4.648	4.641	4 2.955(6)	9 2.884(6)	2.857(6)	10 1.94			11.67
	4-9 4.581	6-10	4.970		6 2.787(5)	10 2.802(5)		17 2.39			
	4-10 4.538	9-10	4.411					19 1.13			
19	4-5'4.295	5'-6	4.349	4.582	4 2.91(4)	6 2.73(3)	2.87(4)	2 2.68			11.18
	4-6 4.697	5'-10	4.642		5'3.13(4)	10 2.69(4)		18 1.13			
	4-10 4.538	6-10	4.970					20 2.32			
20*	4-5'4.295	5'-8'	4.921	4.547	4 2.80	8'2.80	2.80	4 2.20	23	1.59	10.92
	4-8'4.341	5'-10	4.642		5'2.80	10 2.80		16 2.37			
	4-10 4.538	8'-10	4.547					19 2.32			
21	1-5'4.677	5'-7	4.497	4.701	1 2.973(7)	7 2.897(6)	2.890(6)	3 1.61			12.02
	1-7 4.782	5'-9	5.042		5'2.861(6)	9 2.828(6)		8 1.07			
	1-9 4.399	7-9	4.810								
22	2-6 4.698	6-8	4.405	4.714	2 2.834(9)	8 2.823(9)	2.883(9)	5 0.80			12.02
	2-8 4.797	6-9	4.648		6 2.974(8)	9 2.901(8)		10 1.76			
	2-9 4.715	8-9	5.020								
23	3-5 4.610	5-8	4.921	4.686	3 2.854(5)	8 2.883(5)	2.877(5)	13 1.39			12.07
	3-8 4.797	5-10	4.642		5 2.835(5)	10 2.934(5)		20 1.59			
	3-10 4.597	8-10	4.547								

* Empty

Note: Standard errors for I-I are all 0.003-0.004 A. Standard errors of Ag-Ag (unless empty) range from 0.01 to 0.05 A.

5′, 8′, 9′, and 5, 8, 9 with icosahedra at opposite ends (Fig. 4a). (Note that the figure does not show the primes; the two faces are crystallographically equivalent.)

No pair of face-sharing tetrahedra can have an occupancy sum greater than one. This criterion is fulfilled by all pairs of site occupancies. For example, the highest occupancy is that of site Ag16 (Table IV). An Ag^+ ion in this site may jump to one of sites Ag6, Ag17, and Ag20, all of which are empty.

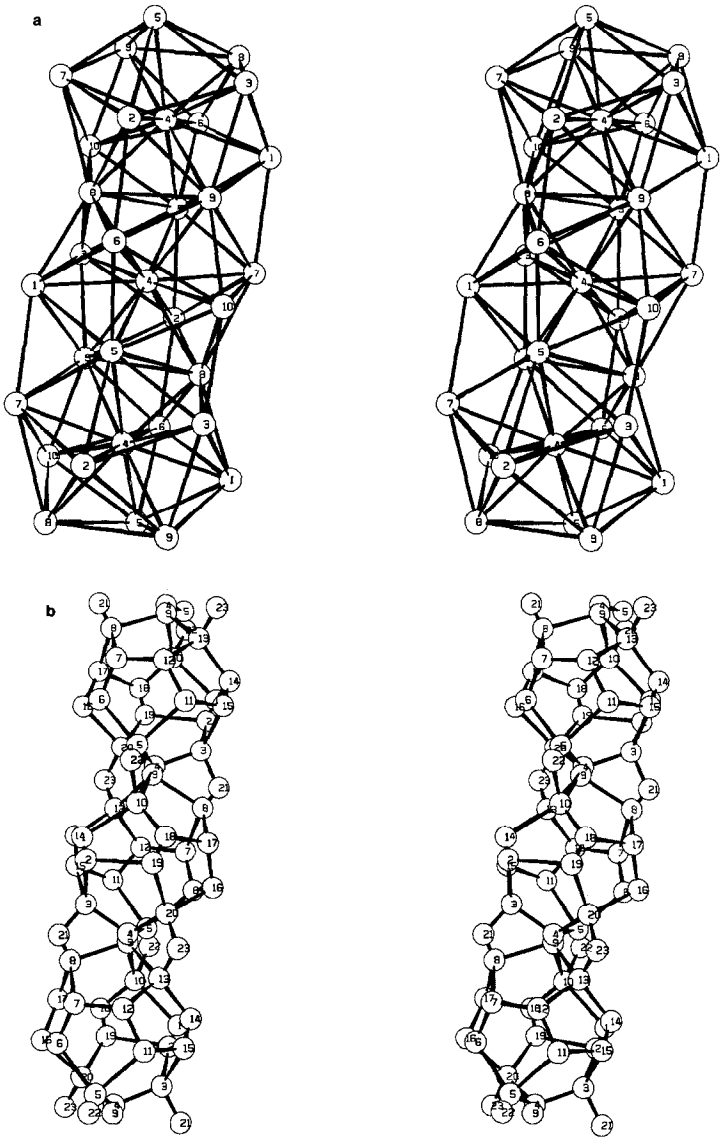

FIG. 4. (a) Stereoscopic drawing of an increment of chain of iodide icosahedra looking almost along the [011] direction. (b) Stereoscopic drawing of possible pathways for the Ag^+ ions. Same aspect and scale as for *a*.

In the iodide tetrahedra surrounding Ag5, Ag8, Ag9, Ag16, and Ag19, one of the Ag–I distances is substantially longer than the average, suggesting that the equilibrium positions of the Ag^+ ions in these sites have closer to three than to four coordinations (Table V). For a regular tetrahedron with edge 4.60 Å, the center-to-corner distance is 2.82 Å and the center-to-plane distance is 0.94 Å. Excluding the tetrahedra about Ag5, 8, 9, 16, and 19, the equilibrium positions in the partially occupied tetrahedra are between 0.09 and 0.21 Å from the centers.

TABLE V

DISTANCES OF SELECTED Ag^+ ION SITES TO NEAREST PLANES

Ag site	Nearest I plane	Distances, Å site-plane
5	2, 8′, 9′	0.13
8	5, 7 , 9	0.36
9	5, 8 , 9	0.04
16	7, 8′, 10	0.54
19	4, 6 , 10	0.38

The volumes (Table IV) of the tetrahedra (see, for example, Ref. (*5*)) range from 10.92 to 12.07 Å^3; the total volume of tetrahedra in the unit cell is 1065.4 Å^3 which is 27.0% of the total crystal volume. The ratio of available sites to charge carriers is 2.875 and the charge-carrier concentration is 0.81×10^{22} cm^{-3}. As given earlier, the isotropic conductivity at room temperature is $1 \times 10^{-4}\ \Omega^{-1}$ cm^{-1}, which leads to $\sigma_1 = 3 \times 10^{-4}$, $\sigma_2 = \sigma_3 \sim 0\ \Omega^{-1}$ cm^{-1} if our prediction that $DMMAg_4I_5$ is a one-dimensional conductor is correct, and $h_m = 0.35$ eV.

For comparison, the values of analogous parameters for the two-dimensional solid electrolyte $Py_5Ag_{18}I_{23}$ (*5*) are as follows: The total volume of the tetrahedra is 31.6% of the unit cell volume, the ratio of available sites to charge carriers is 3.06, the charge-carrier concentration is 0.89×10^{22} cm^{-3}, the conductivity $\sigma_1 = \sigma_2 = 0.017\ \Omega^{-1}$ cm^{-1} (*5*, *18*), $\sigma_3 \sim 10^{-5}$–$10^{-6}\ \Omega^{-1}$ cm^{-1} (*18*), and $h_m = 0.21$ eV (*5*).

The differences in all but the values of h_m cannot account for the enormous difference in conductivity. It is rather the mobility, which contains the Boltzmann factor $\exp(-h_m/kT)$, that does; it is related in a complex way to the nature and number of available pathways which are more favorable in the two-dimensional than in the one-dimensional solid electrolyte.

A comparison of the structure of $DMMAg_4I_5$ should be made with that of piperazinium 10-silver 12-iodide 4-dimethylformamide (*28*). There *appear* to be "one-dimensional" pathways in the latter also. The possible channels are formed by interpenetrating icosahedra (Fig. 5), an arrangement considerably different from that of the icosahedra in $DMMAg_4I_5$ (Figs. 2 and 4). It turns out that although the ratio of face-sharing tetrahedra to Ag^+ ions in the piperazinium compound is 3.00, the Ag^+ ions in the structure are ordered and there is no way for them to have a cumulative net

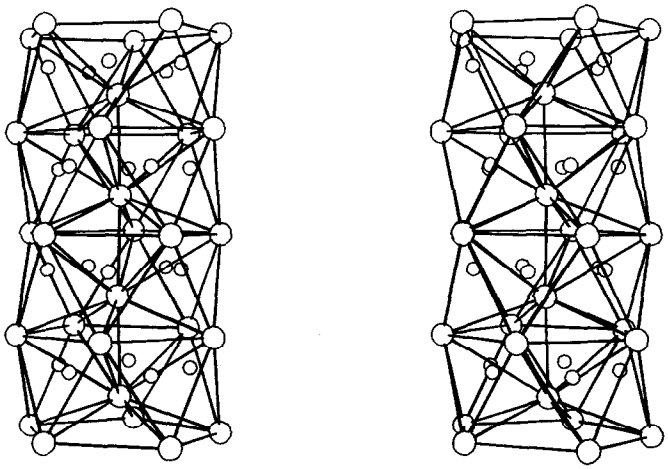

FIG. 5. Stereoscopic view of a two-unit cell increment of the channels formed by the face-sharing iodide tetrahedra in $(C_4N_2H_{12})Ag_{10}I_{12} \cdot 4C_3H_7NO$. The *a* axis points out of the paper. Large spheres are I^- ions, small spheres Ag^+ ions (from Ref. (*23*)).

translation, as shown in detail elsewhere (*28*).

Although it is not possible for the Ag^+ ions in the $(C_4N_2H_{12})Ag_{10}I_{12}\cdot 4C_3H_7NO$ structure to become disordered at a temperature below its decomposition temperature, the structure of $DMMAg_4I_5$ does allow the Ag^+ ions to order at lower temperatures. The most likely ordering is implied by the occupancies shown in Table I. There are eight sites, Ag2, 7, 15, 16, 18, 21, 22, and 23, that have occupancies greater than 0.5. The tetrahedra containing these sites should not and do not share faces (see table IV and Fig. 4).

We obtain the eight sums of the occupancies (Table I) of the sites (Table IV) surrounding each of the above eight sites and add them appropriately to the occupancies of each of the eight sites. These sums are 1.044, 1.074, 1.101, 0.945, 0.966, 0.94, 0.988, and 0.937, respectively. Only one site, Ag19, is shared by two, namely Ag2 and Ag18, and only one site, Ag9, with a low occupancy, 0.100, is not included among the sites contributing to the above sums. Thus one may, with some confidence, predict that if the Ag^+ ions do order, they will move to fill the sites that have the highest occupancy at room temperature.

Unlike the case of $PyAg_5I_6$ (*4*), it does not appear that such ordering will make the Ag^+ ions immobile. In $PyAg_5I_6$, there is a broad heat effect, the peak centered near the temperature at which $PyAg_5I_6$ becomes a true solid electrolyte. The broad peak actually overlaps the temperature at which the Ag^+ ions order (*18*). It remains to be seen whether there is a heat effect in $DMMAg_4I_5$ near the ordering temperature. Still one may argue, as in the case of $PyAg_5I_6$, that even though one would not expect a change in space group, the structure of the $DMMAg_4I_5$ is not the same as that of the disordered one (*29*), and that an order-disorder transition will occur. The temperature below which ordering is complete has not been determined. Resistance measurements down to 240 K continue to give a linear relation between $\log(\sigma T)$ and T^{-1}, showing that at least to this temperature $DMMAg_4I_5$ continues to be a true, though very poor, solid electrolyte.

Finally, we point out that $DMMAg_4I_5$ is the only true one-dimensional solid electrolyte that has thus far been found among all the halogenide solid electrolytes. As expected, it is a poor solid electrolyte, having a high activation enthalpy and low conductivity.

Appendix

Structure of *N,N*-Dimethylmorpholinium Iodide

1. Experimental

The crystal on which the data were taken had a monoclinic morphology with (100), (010), and (001) faces. The longest dimension (0.238 mm) was along [010]; the widths of the (100) and (001) faces were 0.074 and 0.117 mm, respectively. Initial diffraction data were obtained with the Buerger precession camera (Mo$K\alpha$ radiation). Reflections $0k0$ with k odd were absent, indicating $P2_1/m$ and $P2_1$ to be the probable space groups. Initial values of the lattice constants gave a volume which when compared with that allotted to the dimethylmorpholinium iodide in the solid electrolyte implied that the cell content must be two formula units.

The X-ray data were collected with the same type of equipment as for the $DMMAg_4I_5$, Mo$K\alpha$ radiation, $0 \leq 2\theta \leq 60°$, same scan-rate range, same checking. Of a possible 1475 independent reflections observable, 1027 were observed ($I > 3\sigma(I)$) and used in the structure determination and refinement. The measured spacings of 15 reflections were used for the determination of the lattice constants. The results were

$a = 8.861(4)$, $b = 8.020(2)$, $c = 6.685(2)$ Å, $\beta = 101.07(3)°$.

The formula weight of the compound is 243.09, the volume of the unit cell is 466.2(5) Å^3; with $Z = 2$, the calculated density is 1.731 g cm^{-3}. The linear absorption coefficient for Mo$K\alpha$ radiation $\mu = 33.35$ cm^{-1}. Absorption corrections were calculated on the basis of an 8 × 8 × 8 grid. Lorentz-polarization corrections were applied to the observed data.

2. *Determination and Refinement of the Structure*

Because the dimethylmorpholinium ion can have a plane of symmetry, the space group $P2_1/m$ was assumed to be the more likely one. With $Z = 2$, the O, N, and two methyl C's and H's in each ion must then lie in the mirror planes as must the I^- ions. The Patterson plane at $y = \frac{1}{2}$ immediately gave the x and z parameters of the I^- ions. These and isotropic thermal parameters were used in a least-squares calculation, following which the first six peaks of a difference synthesis gave the positions of the independent O, N, and four C atoms. Subsequent least-squares calculations with anisotropic thermal parameters quickly reduced the R value to about 0.03. Hydrogen atoms were subsequently included with C–H distances equal to 1.10 Å. The H positions were not refined, but were recalculated until the positions of the O, N, and C's showed zero shift. The isotropic thermal parameters of the H atoms were all set equal to 5.8 Å^2 and were also kept constant. The final $R = \Sigma||F_o| - |F_c||/\Sigma|F_o| = 0.028$ for the 1027 structure amplitudes. The estimated standard error of an observation of unit weight was 1.06. Positional and thermal parameter values are given in Tables VI and VII, respectively.

3. *Description of the Structure*

As expected, the morpholine part of the *N,N*-dimethylmorpholinium ion (Fig. 6) has the chair form. The two methyl carbons and the two C2 chair atoms bonded to the N form a slightly distorted tetrahedron. All C–N bonds (Table VIII) are equal to 1.50 Å within ±0.01-Å limits of error (±3σ limits of error are used in this discussion). This is 0.03 Å greater than the value expected from the tetrahedral radii. However, it seems that the larger distances occur often. This was recognized (*30*) a long time ago. More recent examples with estimated standard errors comparable to those of the present work are not easy to find in the literature. However, several can be found with the same central value of 1.50 Å. One example is $[(CH_3)_3NH]_3Mn_2Cl_7$ (*31*), in which the C–N distances equal 1.50 Å within ±0.03 Å. The C2–C4 distance, 1.50 ± 0.01 Å (Table VIII), does appear to be short and the C4–O distance, 1.42 ± 0.01 Å, is close to the ideal single-bond value of 1.43 Å.

A projection of the structure down the *b*

TABLE VI

DMMI, POSITIONAL PARAMETERS, AND B_{eqv}

Atom	x	y	z	B_{eqv} (Å^2)
I	0.20209(4)	0.250	0.19898(5)	4.019(5)
N	0.7774(3)	0.250	0.4898(4)	3.26(7)
C1	0.6375(5)	0.250	0.5853(6)	4.4(1)
C2	0.7818(3)	0.0980(4)	0.3595(4)	4.17(7)
C3	0.9165(5)	0.250	0.6591(6)	4.9(1)
C4	0.6559(4)	0.1036(4)	0.1732(4)	5.43(8)
O	0.6678(4)	0.250	0.0566(4)	6.61(9)
H11	0.534	0.250	0.465	5.8
H12	0.638	0.138	0.680	5.8
H31	1.021	0.250	0.594	5.8
H32	0.915	0.362	0.754	5.8
H21	0.767	-0.014	0.449	5.8
H22	0.894	0.092	0.312	5.8
H41	0.665	-0.007	0.079	5.8
H42	0.544	0.103	0.221	5.8

Note: For this case, $B_{eqv} = (4/3)*\{a^2*Beta(1,1) + b^2*Beta(2,2) + c^2*Beta(3,3) + 2*a*c*Beta(1,3)*cosBeta\}$

TABLE VII

DMMI, THERMAL PARAMETERS, U_{ij}

Name	U(1,1)	U(2,2)	U(3,3)	U(1,2)	U(1,3)	U(2,3)
I	0.0490(1)	0.0507(1)	0.0539(1)	0.000	0.0123(1)	0.000
N	0.051(2)	0.041(2)	0.031(2)	0.000	0.006(1)	0.000
C1	0.061(2)	0.073(3)	0.038(2)	0.000	0.018(2)	0.000
C2	0.064(2)	0.044(2)	0.051(2)	0.001(2)	0.013(1)	-0.011(1)
C3	0.057(3)	0.067(3)	0.051(3)	0.000	-0.014(2)	0.000
C4	0.083(2)	0.076(2)	0.046(2)	-0.009(2)	0.009(2)	-0.024(2)
O	0.094(2)	0.128(3)	0.028(1)	0.000	0.010(2)	0.000

axis is shown in Fig. 7. We would assert that the H atoms are, at least, very close to their correct positions. Even if this were incorrect, there could still not be significant van der Waals interaction between DMM ions. The closest approach, 3.41 Å of H atoms, is that of 2H12 of one ion to 2H11 of the other. Along b, there is an H21–H21 intermolecular distance of 4.23 Å. These are considerably longer than the van der Waals diameter, 2.4 Å (*32*), of H.

Each iodide ion "looks" at the two N atoms past methyl groups (Fig. 7). If we focus our attention on the I^- ion nearest 0, 0, 0 (as opposed to 1, 1, 1), lying in the plane $y = \frac{1}{4}$, these two nearest N atoms are in the DMM ions in the planes $y = \frac{3}{4}$ and $y = -\frac{1}{4}$ and are at a distance 4.505(4) Å. The next nearest N is in the DMM ion in the unit cell to the left, which we designate the $(-++)$ cell, and is in the plane $y = \frac{1}{4}$; the distance is 4.56(1) Å. The distance to the N

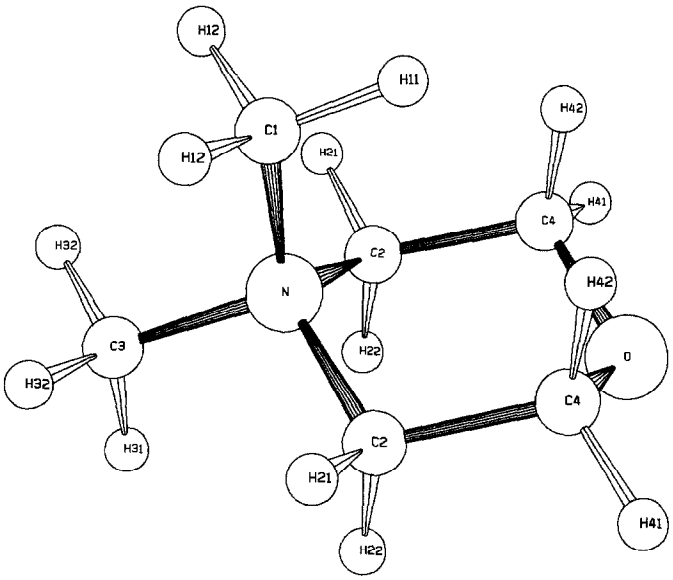

FIG. 6. *N,N*-Dimethylmorpholinium ion.

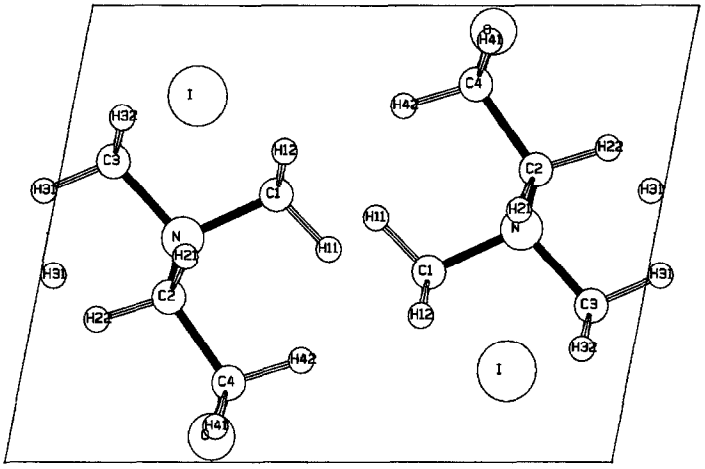

FIG. 7. Projection of the structure of DMMI down the *b* axis.

atom in $y = \frac{1}{4}$ of the DMM ion in the same unit cell (+ + +) is 5.10 Å. These five DMM ions may interact electrostatically with the particular I^- ion, considering that the positive charge of the DMM ion is near the N atom.

There are also at least van der Waals interactions between the I^- ion and the H atoms. Moving clockwise from the unit cells (+ + −) and (+ − −) are the following I^-–H distances: H41, 3.08 Å in each of (+ + −) and (+ − −); H42, 3.23 Å and H11, 3.13 Å in the DMM at $y = \frac{1}{4}$ in (+ + +); H12, 3.45 Å in each of (+ + +) and (+ − +); H31, 3.34 Å in (+ + +), but belonging to the DMM at $y = \frac{1}{4}$ in (− + +), H22, 3.23 Å in (− + +); H32 in each of (+ + +) and (+ − +). All these distances are less than or equal to the sum of the I^- radius and the H van der Waals radius 2.25 and 1.2 Å, respectively. Seven DMM ions are involved in this bonding.

TABLE VIII

INTERATOMIC DISTANCES (Å) AND ANGLES (°) IN THE *N,N*-DIMETHYLMORPHOLINIUM ION

Bond distances		Bond angles	
N -C1	1.499(5)	C1-N-C2	111.3(2)
-C2	1.503(3)	C1-N-C3	107.7(3)
-C3	1.505(5)	C2-N-C2′	108.4(3)
C2-C4	1.505(4)	C2-N-C3	109.1(2)
C4-O	1.424(4)	N-C2-C4	110.9(3)
		C2-C4-O	110.9(3)
		C4-O-C4′	110.9(3)
Non-bonded distances			
N -C4	2.478(4)	C2-C3	2.450(5)
N -O	2.872(5)	C2-C4	2.826(5)
C1-C2	2.478(4)	C2-O′	2.413(4)
C1-C3′	2.426(6)	C4-C4′	2.348(7)
C2-C2′	2.438(6)		

Note: See Fig.6 for carbon atom identification

Acknowledgments

This work was supported by the National Science Foundation under Grant DMR-810305 through the Ceramics Program of the Division of Materials Research. S. G. thanks the Council of Research and Creative Work of the University of Colorado for a fellowship for the academic year 1985–1986 during which this work was carried out. We thank R. C. Haltiwanger for collecting the diffraction data.

References

1. S. GELLER, *Science* **157,** 310 (1967).
2. H. WIEDERSICH AND S. GELLER, *in* "Chemistry of Extended Defects in Non-Metallic Solids" (L. Eyring and M. O'Keefe, Eds.), pp. 629–650, North-Holland, Amsterdam (1970).
3. S. GELLER AND M. D. LIND, *J. Chem. Phys.* **52,** 5854 (1970).
4. S. GELLER, *Science* **176,** 1016 (1972); S. GELLER AND B. B. OWENS, *J. Phys. Chem. Solids* **33,** 1241 (1972).
5. S. GELLER AND P. M. SKARSTAD, *Phys. Rev. Lett.*

33, 1484 (1974); S. GELLER, P. M. SKARSTAD, AND S. A. WILBER, *J. Electrochem. Soc.* **122,** 332 (1975).
6. S. GELLER, *Phys. Rev. B* **14,** 4345 (1976).
7. J. COETZER, G. J. KRUEGER, AND M. M. THACKERAY, *Acta Crystallogr. Sect. B* **32,** 1248 (1976).
8. M. M. THACKERAY AND J. COETZER, *Acta Crystallogr. Sect. B* **32,** 2197 (1976).
9. M. M. THACKERAY AND J. COETZER, *Acta Crystallogr. Sect. B* **32,** 2966 (1976).
10. L. Y. Y. CHAN AND S. GELLER, *J. Solid State Chem.* **21,** 331 (1977).
11. L. Y. Y. CHAN AND S. GELLER, *J. Solid State Chem.* **25,** 85 (1978).
12. M. M. THACKERAY AND J. COETZER, *Acta Crystallogr. Sect. B* **34,** 71 (1978).
13. S. GELLER, J. R. AKRIDGE, AND S. A. WILBER, *Phys. Rev. B* **19,** 5396 (1979).
14. S. GELLER, J. R. AKRIDGE, AND S. A. WILBER, *J. Electrochem. Soc.* **127,** 251 (1980).
15. S. GELLER AND T. SAKUMA, *J. Solid State Chem.* **50,** 256 (1983).
16. S. GELLER AND X. SISHEN, *J. Solid State Chem.* **63,** 316 (1986).
17. J. M. GAINES AND S. GELLER, *J. Electrochem. Soc.* **133,** 1501 (1986).
18. T. HIBMA, *Phys. Rev. B* **15,** 5797 (1977).
19. S. GELLER, A. K. RAY, AND K. NAG, *J. Solid State Chem.* **48,** 176 (1983).
20. S. GELLER, S. A. WILBER, G. F. RUSE, J. R. AKRIDGE, AND A. TURKOVIČ, *Phys. Rev. B* **21,** 2506 (1980).
21. W. B. SMITH AND B. A. SHOULDERS, *J. Phys. Chem.* **69,** 579 (1965).
22. S. S. WILKS, "Mathematical Statistics," Princeton Univ. Press, Princeton, NJ (1946); E. WHITTAKER AND G. ROBINSON, "The Calculus of Observations," Blackie, London (1958).
23. S. GELLER, *Acc. Chem. Res.* **11,** 87 (1978).
24. For example, S. GELLER, J. B. JEFFRIES, AND P. J. CURLANDER, *Acta Crystallogr. Sect. B* **31,** 2770 (1975).
25. S. GELLER, *Acta Crystallogr.* **14,** 1026 (1961).
26. S. GELLER AND J. KATZ, *Bell System Tech. J.* **41,** 425 (1962).
27. "International Tables for X-Ray Crystallography" (T. Hahn, Ed.), pp. 196–197, Reidel, Dortdrecht (1983).
28. S. GELLER, L. Y. Y. CHAN, AND G. F. RUSE, *Mater. Res. Bull.* **13,** 339 (1978).
29. S. GELLER *in* "Solid Electrolytes, Topics in Applied Physics" (S. Geller, Ed.), Vol. 21, pp. 41–66, Springer-Verlag, Heidelberg/New York (1977).
30. J. L. HOARD, S. GELLER, AND T. B. OWEN, *Acta Crystallogr.* **4,** 405 (1951), and references therein.
31. R. E. CAPUTO, S. ROBERTS, R. D. WILLETT, AND B. C. GERSTEIN, *Inorg. Chem.* **15,** 820 (1976).
32. L. PAULING, "The Nature of the Chemical Bond," p. 260, Cornell Univ., Ithaca, NY (1960).